

STM Studies of TbTe_3 : Evidence for a Fully Incommensurate Charge Density Wave

A. Fang,¹ N. Ru,¹ I. R. Fisher,¹ and A. Kapitulnik^{1,2}

¹Department of Applied Physics, Stanford University, Stanford, California 94305, USA

²Department of Physics, Stanford University, Stanford, California 94305, USA

(Received 19 January 2007; published 23 July 2007)

We observe unidirectional charge density wave (CDW) ordering on the quasi-2D material TbTe_3 with a scanning tunneling microscope at ~ 6 K. Our analysis indicates that the CDW is fully incommensurate, with wave vector $q_{\text{CDW}} \approx 0.71 \times 2\pi/c$. By imaging at various tip-sample voltages, we highlight effects of the subsurface layer and its effect on the CDW. We also observe an additional (possibly surface) dimerization and $\approx 0.68 \times 2\pi/a$ ordering perpendicular to the CDW.

DOI: 10.1103/PhysRevLett.99.046401

PACS numbers: 71.45.Lr, 61.44.Fw, 68.37.Ef

STM as a real-space local probe is ideal for studying systems with multiple interacting periodicities, as both the wave vector and phase information can be obtained. This is crucial for distinguishing electronic effects from the lattice. The quintessential case is charge density wave (CDW) systems, which can have many different mechanisms for charge corrugation. Weakly interacting systems are predominantly driven by Fermi surface (FS) nesting, where a single vector $q_{\text{CDW}} = 2k_f$ connects points on the FS. Although prototypical CDW's form in 1D systems, in 2D, nesting is also possible if the FS has parallel regions. The rare-earth tritelluride series $R\text{Te}_3$ (R = rare-earth) is such a quasi-2D system; however, it is the first case where the (nominal) in-plane fourfold crystal symmetry is broken and a unidirectional [1] (as opposed to 2D) CDW forms [2]. From a symmetry perspective, it is analogous to stripes in the high- T_c superconductors, without the complications from disorder.

The CDW was first detected by transmission electron microscopy (TEM) [3] and later by x-ray diffraction (XRD) [4–6] and angle-resolved photoemission spectroscopy (ARPES) [7,8]. Yao *et al.* [9] showed, by modeling a single Te square net, that under the given conditions unidirectional CDW formation is favored. This model fits the measured bands well [8] and favors a *single* nesting along the diagonal of the net, with $q_{\text{CDW}} \approx (0.75, 0.75) \times \pi/a_0$, where a_0 is the Te-Te spacing of 3.1 Å. However, additional periodicities in the real crystal structure create difficulties in interpreting measurements. $R\text{Te}_3$ contains double layers of nominally square Te planes (where the CDW resides) separated by $R\text{Te}$ block layers [10]. The adjacent block layer has in-plane basis vectors (**a**, **c**) that are 45° to the Te net and $\sqrt{2}$ times longer than a_0 [11]. The strength of coupling to this additional periodicity folds an according amount of spectral weight from the original bands back into the reduced Brillouin zone (3DBZ) [8]. This creates additional nesting possibilities between the original and folded bands, as depicted in Fig. 1(a). For diffraction measurements such as XRD, the wave-vector is ambiguous within a reciprocal lattice vector, and is often reported

inside the reduced 3DBZ as $q_{\text{CDW}} \approx 2/7 \times 2\pi/c$. This ambiguity regarding which modulation is the dominant contribution to the CDW shows up elsewhere in the literature, e.g., the $3/4$ vs $1/4$ modulation seen in Na-CCOC [12]. This periodicity also affects determination of the CDW structure, i.e., whether it is incommensurate, dis-

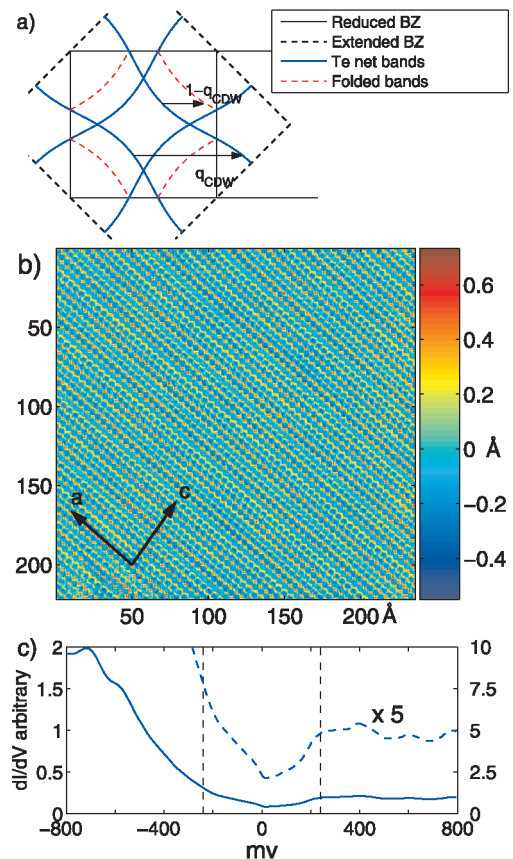


FIG. 1 (color). (a) Schematic of band folding and nesting in $R\text{Te}_3$. (b) $T \approx 6$ K topography with voltage bias +200 mV, 50 pA current. (c) Average spectrum in the range ± 800 mV. Spectrum also multiplied to show gap structure. Lines indicate maximal gap as measured by ARPES.

commensurate, etc., which is important for determining the strength of the lattice interaction.

In this Letter, we use scanning tunneling microscopy and spectroscopy to study the unidirectional CDW system TbTe_3 . By taking large area scans at different bias voltages, we can separate out the lattice effects from the CDW and discuss how it has affected previous interpretations of the CDW structure. Using a combination of real-space and Fourier analysis, we find that the CDW is in fact fully incommensurate. We also note two new surface effects in this material: dimerization and a second charge ordering with a perpendicular component to the CDW.

We performed measurements on a homemade UHV cryogenic STM. Single crystals were grown using a self-flux method as previously reported [13]. The samples were cleaved between the two Te planes in $<2 \times 10^{-10}$ Torr vacuum and quickly lowered to the ~ 6 K section of the microscope, where cryopumping ensures that the surface remains free from adsorbates. Topography was taken at several bias voltages ($=V_{\text{sample}} - V_{\text{tip}}$) and 50 pA setpoint current. Scan sizes were as large as $\sim 240 \times 240 \text{ \AA}^2$. While surfaces often had large areas with no obvious surface impurities (which might pin the CDW); flakes or other “dirt” every few hundred \AA limited the maximum size of our scans. Thermal compensation, hysteresis minimization techniques, and postprocessing were used to reduce the amount of scan distortion in the images. An example of such a scan with bias voltage $+200$ mV is shown in Fig. 1(b). We also took spectroscopic scans over smaller areas, i.e., a dI/dV [proportional to the local density of states (DOS)] spectrum at every point with a lock-in amplifier. The spectra mainly had spatial variations relating to the lattice and CDW; thus, we show in Fig. 1(c) an averaged spectrum taken in the range of ± 800 mV. ARPES has shown a partially gapped FS with maximal gap of 240 mV [14]. As expected, we see a depressed DOS inside the gap with finite conductance at zero bias. A possible reason for the high conductance at negative energies is that we are also probing the filled p_z orbitals of the Te atoms, where it is easier to remove electrons than add them.

CDWs appear in STM topography; however, a different sample bias may give different results depending on how many of the states responsible for the CDW are integrated. Figure 2(a) shows a (zoomed-in) scan at -800 mV and 50 pA, a voltage outside the gap which should include all the states responsible for CDW formation. We observe the square lattice of the surface Te layer, with a Te-Te (average) spacing of $\approx 3 \text{ \AA}$. The atomic features visually swamp any CDW modulation. One possible explanation for its relatively small amplitude is that the extended nature of the p_z orbitals causes the tip to be further away from where the CDW wave functions exist. Since the CDW wave function decays exponentially out of the plane [15], its contribution to the topography is expected to be small. The second is that it is energetically unfavorable to have large charge inhomogeneities due to Coulomb repulsion, and

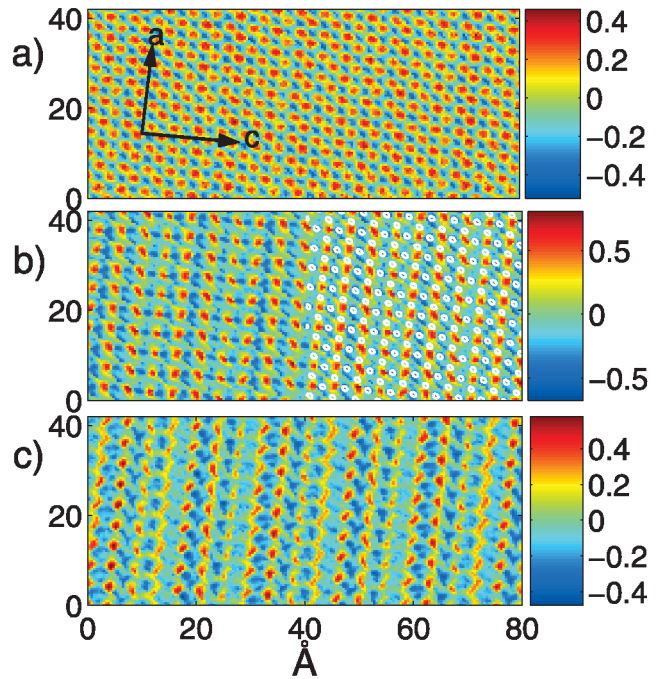


FIG. 2 (color). Zoomed-in view of topographic scans with 50 pA setpoint current. All units in \AA . (a) Topography at -800 mV, (b) -200 mV. Right half shows locations of the surface Te atoms. (c) $+200$ mV.

thus when looking at quantities that are closer to representing total charge, i.e., large bias voltages, the CDW amplitude appears small.

We also see dimerization, with pairs of atoms connected in an upper-left, lower-right direction. This indicates another broken symmetry, as it chooses a direction 45° (as opposed to -45°) to the CDW. Although the Te net is expected to be unstable against a 3.1 \AA bond length [16], this effect has not been directly observed by XRD. However, it is consistent with the bimodal bond length distribution found by the atomic pair distribution function (PDF) analysis of powder x-ray data [17]. We do not see a complex pattern of oligomers as proposed in the works of Malliakas *et al.* [4], since the simple two-atom dimers have a repeating pattern of long and short bonds within a row. This is also suggested in Fig. 3(b) (red line) by a lack of lower frequency components in the Fourier transform. Although what we see may be a surface effect, this should prompt a reexamination of the $R\text{Te}_3$ crystal structure.

To probe the sample more closely, we decrease the bias voltage to -200 mV ($< \Delta_{\text{max}}$), which causes the tip to move 3 \AA closer to the sample. Because of the partially gapped FS, we still expect to see states responsible for CDW formation at these lower energies. The CDW signal is slightly stronger; however, now we note a new, larger square lattice rotated 45° . This new periodicity has three potential causes: Dimerization (as noted above), the block layer (as mentioned earlier), and stacking of the pair of Te layers deeper in the sample, which results in two crystallo-

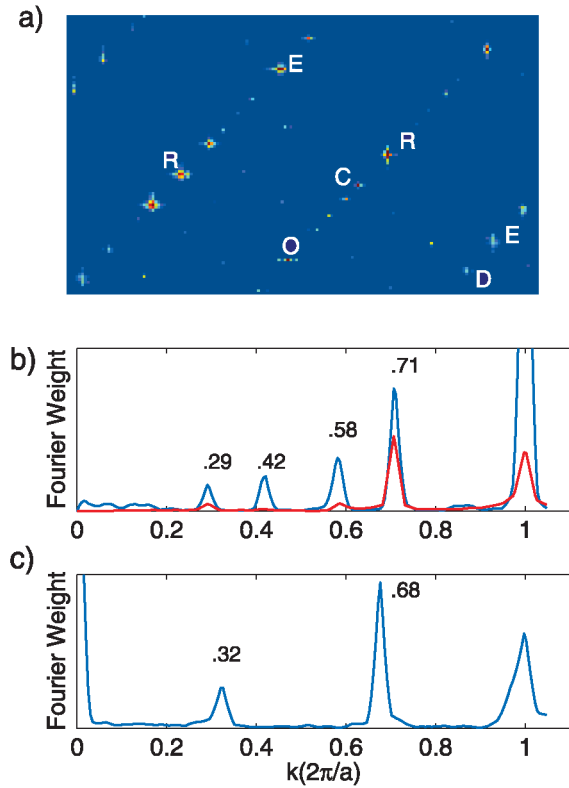


FIG. 3 (color). (a) Fourier transform of +200 mV topography [Fig. 1(a)]. O = Origin; E = Te square lattice (2D BZ); R = block layer (3DBZ). (b) Blue: Line cut from O to R, thru the CDW. Red: same analysis for -800 mV topograph. Amplitude rescaled for clarity. (c) Line cut from the CDW point C to D.

graphically inequivalent Te atoms at the surface. These mechanisms all have the same wave-vector for their superlattice, so to tell them apart we note that they have different registry to the surface Te atoms (i.e., phase). The peaks of the superlattice fall between two Te atoms, four Te atoms, or on every other Te atom, respectively. Thus we look at the phase of the Fourier peaks for the Te lattice combined with the spectroscopic data. The locations of the surface Te atoms are depicted as white circles in the right half of Fig. 2(b). Since the red spots fall between four Te atoms, this suggests that we are imaging effects from the Tb atoms in the block layer. Seeing effects from the next layer below is not unheard of in STM, e.g., graphite [18].

To further bring out the CDW features, we use +200 mV, as shown in Fig. 2(c). According to the spectra, the lower density of states at positive bias suggests that the tip is even closer to the sample. The irregular shapes of the “atoms” are likely due to the convolution of the true sample topography with tip states. This set of data shows most strongly the CDW ordering and effects of the block layer.

To understand the structure of the CDW, we compare the Fourier transforms of the +200 mV and -800 mV topographies. In Fig. 3(a) (+200 mV) the Fourier points from the Te net are clearly seen, as well as those of the block

layer. Figure 3(b) (blue line) is a line cut showing five peaks—the superlattice at $2\pi/c$, and four intermediary peaks at $0.29, 0.42, 0.58,$ and $0.71 \pm 0.02 \times 2\pi/c$. In another interpretation, Kim *et al.* [17] identified these peaks as satellites from discommensurations [19]. However, the -800 mV data [Fig. 3(b) red line] show that $q_{\text{CDW}} = 0.71$ is the “true” CDW wave vector, and that the other peaks are greatly reduced. Thus they are not representative of an intrinsically discommensurate structure, as they do not exist under different tunneling conditions. Rather, we identify them as $0.29 = 1 - q, 0.42 = 2q - 1,$ and $0.58 = 2 - 2q$ which is mixing between q and the block layer superlattice. In real space, this amounts to distortions of STM DOS measurements due to the subsurface layer and measurement conditions. This distortion seems to increase when the superlattice point is stronger, as in the blue line. Because q_{CDW} is outside the 3DBZ, we conclude that nesting primarily occurs between the original unfolded bands and that block layer coupling is weak.

In our data, the Fourier peaks are narrow, indicating a long coherence length for the modulations. Additional width to the peaks comes from a combination of scan distortion, spectral leakage [20], and some variation in the CDW amplitude, possibly due to defects below the surface. Overall, our interpretation that the true CDW has little harmonic content and a long coherence length is consistent with XRD [5] which shows a nearly perfectly sinusoidal lattice modulation in the bulk.

Having ruled out a discommensurate structure, next we check if the CDW is fully incommensurate or commensurate against the nearest fraction of $5/7$ ($= 0.714$). (Although it is difficult to distinguish incommensurate against a high denominator fraction commensurate.) We check our low temperature data for commensuration against $5/7$ by filtering out features perpendicular to the CDW, then taking a line cut in the direction of the CDW wave vector in real space. Next we match up groups of 7 unit cells. If the CDW were commensurate, all the groups would be identical. This analysis technique, which checks for CDW registry to the lattice, is immune to scan distortions and can determine the wave vector of a CDW to higher precision than simple Fourier analysis. Figure 4(a) shows the results, with the arrow pointing at a region of evolution from one group to the next. From this, we conclude that the CDW is incommensurate. Figure 4(b) is the same data, with the lattice filtered out. A $\sim 5/7$ modulation can clearly be seen, with some distortion caused by the lattice positions as previously noted. Figure 4(c) shows the Fourier filtered component for the CDW slowly advancing as expected for slight incommensuration with $q < 5/7$ [21]. This value of q means that the four peaks in Fig. 3(b) (blue line) are not evenly spaced, but rather the two center peaks are slightly spread apart. Likewise, in the work of Kim *et al.* [17] the two center peaks are slightly closer together, consistent with $q > 5/7$ in CeTe_3 [6].

It is not unexpected that the CDW is incommensurate since ARPES has shown that it is FS nesting driven [8].

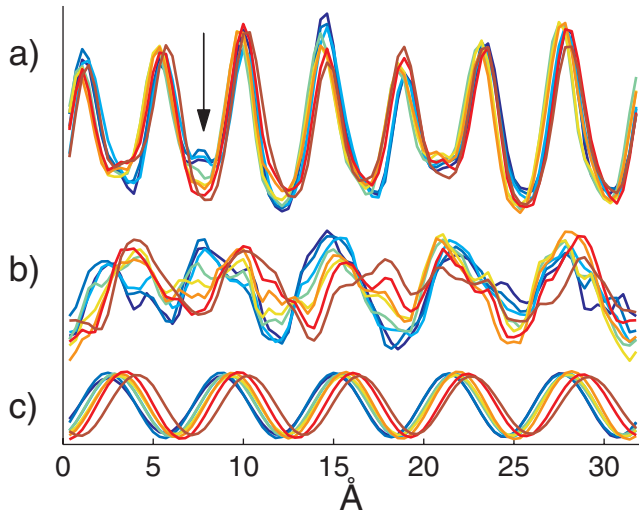


FIG. 4 (color). (a) Line scan along the sample (CDW + lattice), in groups of 7 unit cells. Blue is one end of the sample, evolving to dark red (other end). (b) Same signal, with atomic features filtered out (CDW + distortions), and amplitude multiplied by 2. (c) Main CDW component only.

Recent x-ray data also show incommensuration in the bulk at room temperature with $q = 0.704 \pm 0.001$ [5]. However, it is well known that incommensurate CDWs can change their wave vector as a function of temperature [6] or even undergo a change to the discommensurate or commensurate structure [19]. There may also be surface effects which make the CDW different than in the bulk [22]. However, resistivity measurements do not indicate any transitions from room temperature down to 1.8 K [5]. The fact that it stays incommensurate through this entire range supports the notion that the high order denominator (≥ 7) for the nearest commensuration fractions makes any lattice locking effects weak [23].

Finally, we note weak Fourier signals at $(q_c, q_a) \approx (0.71, 0.68)$, as satellites perpendicular to the CDW. Figure 3(c) shows a line cut in the direction from C to D. This means that there is a $\approx 1.5 \times a$ modulation along the crests of the CDW, and that each row of the CDW is shifted laterally with respect to the next. This signal is not seen in room temperature x-ray diffraction, meaning that it is possibly a previously unobserved second CDW phase transition at low temperature or a surface reconstruction effect [24].

In conclusion, we show that TbTe_3 has a unidirectional CDW at low temperatures, with a dominant wave vector $q = 0.71$, implying weak block layer coupling and nesting in the extended zone. Yet this block layer strongly affects measurements by acting as an additional periodicity which distorts STM data. However, by tuning the tunneling parameters, these effects can be separated out. By combining Fourier and real-space analysis, we find that the CDW is fully incommensurate with long coherence length. The

CDW's commensuration appears unaffected by the lattice at all temperatures. Thus RTe_3 could be an ideal model system to study in which correlations, saddle Fermi surface effects, and disorder all compete to form a new broken symmetry state, which can then be tested using new theories invented to investigate such states [25]. Finally, we observe two new (possibly surface) effects: dimerization and another ordering with a perpendicular component to the CDW.

We thank S. Kivelson, H. Yao and E. A. Kim for useful discussions. STM work supported by the U. S. DoE under contract No. DE-FG03-01ER45925. The crystal growth was supported by the U. S. DoE under contract No. DE-AC02-76SF00515.

Note added in proof.—Recently, the second, lower temperature phase transition was observed by XRD and ARPES perpendicular to the CDW with wave vector ≈ 0.68 in ErTe_3 [24].

- [1] We refer to the CDW as unidirectional instead of 1D to differentiate it from CDWs that exist in linear chain compounds.
- [2] The full crystal structure has a tiny orthorhombic distortion which only chooses the direction of the CDW, but does not affect it in terms of being unidirectional or bidirectional.
- [3] E. DiMasi *et al.*, Phys. Rev. B **52**, 14 516 (1995).
- [4] C. Malliakas *et al.*, J. Am. Chem. Soc. **127**, 6510 (2005).
- [5] N. Ru *et al.*, arXiv:cond-mat/0610319.
- [6] C. Malliakas and M. Kanatzidis, J. Am. Chem. Soc. **128**, 12 612 (2006).
- [7] G.-H. Gweon *et al.*, Phys. Rev. Lett. **81**, 886 (1998).
- [8] V. Brouet *et al.*, Phys. Rev. Lett. **93**, 126405 (2004).
- [9] H. Yao *et al.*, Phys. Rev. B **74**, 245126 (2006).
- [10] B. Norling and H. Steinfink, Inorg. Chem. **5**, 1488 (1966).
- [11] RTe_3 , the **b** axis is perpendicular to the Te plane.
- [12] T. Hanaguri *et al.*, Nature (London) **430**, 1001 (2004).
- [13] N. Ru and I. Fisher, Phys. Rev. B **73**, 033101 (2006).
- [14] V. Brouet (private communication).
- [15] W. Sacks *et al.*, Phys. Rev. B **57**, 13 118 (1998).
- [16] R. Patschke and M. Kanatzidis, Phys. Chem. Chem. Phys. **4**, 3266 (2002).
- [17] H. Kim *et al.*, Phys. Rev. Lett. **96**, 226401 (2006).
- [18] W. Pong and C. Durkan, J. Phys. D **38**, R329 (2005).
- [19] R. Thomson *et al.*, Phys. Rev. B **38**, 10 734 (1988).
- [20] The Fourier weight of a signal with a single frequency is spread out when a noninteger number of periods resides within the scan range. Care must be taken when Fourier filtering and then reverse transforming, as done in Fig. 4.
- [21] We can do a similar analysis to show that $q > 7/10$. Thus $0.700 < q < 0.714$.
- [22] S. Brown *et al.*, Phys. Rev. B **71**, 224512 (2005).
- [23] G. Gruner, *Density Waves in Solids* (Perseus, Cambridge, MA, 1994).
- [24] N. Ru and R. Moore (unpublished).
- [25] J. Robertson *et al.*, Phys. Rev. B **74**, 134507 (2006).